Numerical simulation of sea breezes with vertical wind shear during dry season at Cape of Three points, west Africa

S. Cautenet, R. Rosset

Numerical Simulation of Sea Breezes with Vertical Wind Shear during Dry Season at Cape of Three Points, West Africa

S. CAUTENET

Laboratoire de Physique de l'Atmosphère, Université d'Abidjan, Abidjan, Côte d'Ivoire

R. ROSSET

Université-Blaise Pascal, LAMP/OPGC, Aubière, France

(Manuscript received 22 February 1988, in final form 18 July 1988)

ABSTRACT

The airflow over Cape of Three Points (Gulf of Guinea: 4.5°N, 2°W) has been simulated using a three-dimensional mesoscale model in order to investigate the sea breeze developing in synoptic vertical wind shears during the 1979 dry season. Two different meteorological situations, characterized by two contrasted wind profiles between 500 and 2000 m have been studied, with two types of transitions between the lower circulation (SW monsoon) and the upper African easterly jet (AEJ). The first one is a veering case (6 January) and the second is a backing case (23 January). Calculations of CAPE (convective available potential energy) show that whereas instability is a maximum at both sides of the cape, the site of enhanced convection is determined by the wind shear in the 500–2000 m layer. Numerical results confirm satellite observations.

1. Introduction

This paper mainly deals with the numerical modeling of equatorial sea breezes. Mahrer and Pielke's (1978) three-dimensional mesoscale model has been run to simulate two different typical breeze situations along the Gulf of Guinea around the Cape of Three Points (CTP hereafter) about 4.5°N, 2°W. The domain of simulation with its main towns is displayed in Fig. 1, together with its location on the African continent. Sea breezes are constantly observed every day during the dry season, with cloud lines at the breeze front paralleling the coastline from Liberia in the west to the mouth of the Niger river in the east, along a distance of more than 2000 km; examples are displayed in Figs. 2 with Meteosat pictures in the visible range for the 2 days under study (1430 LST 6 January 1979 in Fig. 2a and 1530 LST 23 January 1979 in Fig. 2b). This region around CTP is endowed with unique general as well as local features regarding sea breeze circulations. These equatorial sea breezes develop in the presence of an evanescent Coriolis force (Hong Yan and Anthes 1987). During the dry season, from December to March, the coastline of the Gulf of Guinea (about 5°N) lies in the B or C zone in Walker's diagram (Fig. 3), with the intertropical convergence zone (ITCZ) close

to the coast. In this regime, sea breezes develop within a synoptically sheared flow, between a weak regular southwesterly monsoon flow near the surface and the African easterly jet (AEJ) located at this time of the year between 600 and 800 hPa (Burpee 1972; Rennick 1976).

In spite of flat orography (Fig. 1), this region around CTP displays remarkable climatological rainfall gradients (Fig. 4), about 15 mm km^{-1} in annual values, even reaching 6 mm km^{-1} in May (Trewartha 1961). These gradients are reflected in contrasts of the vegetation cover (Fig. 5), with dense forests of tall trees at the west of CTP whereas the eastern part mainly consists of savannahs. In addition to roughness differences arising from these vegetation covers, Trewartha (1961) suggests that strong gradients in the coastal sea surface temperatures explain the climatological peculiarities observed at CTP; an example is given in Fig. 6 for the first 3 months of 1979, at the four stations of Abidjan, Axim, Takoradi and Accra. Further interest in sea breeze circulations lies in the coastline consisting of straight segments (Fig. 1), oriented at various angles relative to the southwesterly low-level monsoon flux, with a succession of bays and capes locally generating divergence and convergence flow patterns. Such a general convergence pattern can be seen at CTP, but with convective clouds preferentially developing on the west or east coast of the cape, according to day-to-day modulations of the synoptic flow characteristics (veering or backing between the surface and the AEJ).

Corresponding author address: Sylvie Cautenet, Faculté des Sciences, Laboratoire de Physique de l'Atmosphère, (04) BP 322 ABIDJAN (04), Côte d'Ivoire (Ivory Coast), West Africa
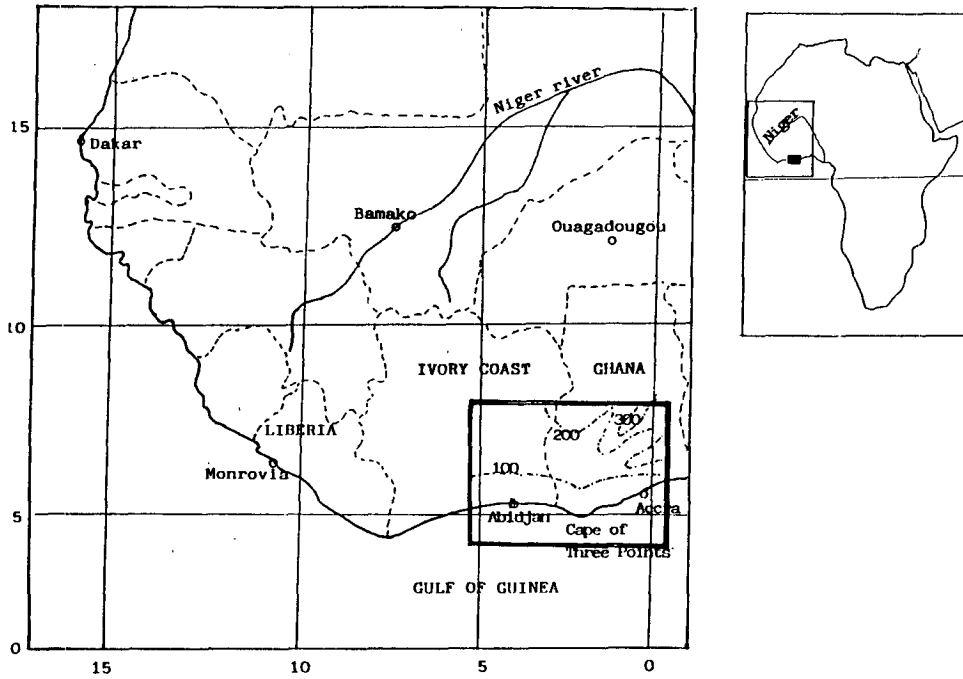
FIG. 1. Location of the domain of simulation at Cape of Three Points (4.5°N, 2°W) in West Africa.
(Topography of the domain is given in meters in dashed-dotted lines.)

Our purpose here is to compare these observed cloud fields as depicted through satellite radiance isocontours (i.e., cloud top heights) with the model-generated vertical velocity patterns.

2. The numerical model

Trewartha (1961) hypothesizes nonhomogenous surface forcing (sea surface temperatures, vegetation covers, convex/concave coastline shape) as the cause of the climatological anomalies observed at CTP. Thus, the model to be adopted must be able to simulate such effects in addition to sheared synoptic flows. The decision was made to use Mahrer and Pielke's numerical model; a detailed description can be found in Mahrer and Pielke (1978). The domain of simulation, a 420 km by 360 km rectangle, is displayed in Fig. 5, with a horizontal grid size $\Delta x = \Delta y = 20$ km. It comprises 11 unevenly spaced levels in the vertical at 5, 15, 100, 300, 700, 1200, 2000, 3000, 4000, 5000, and 6000 m.
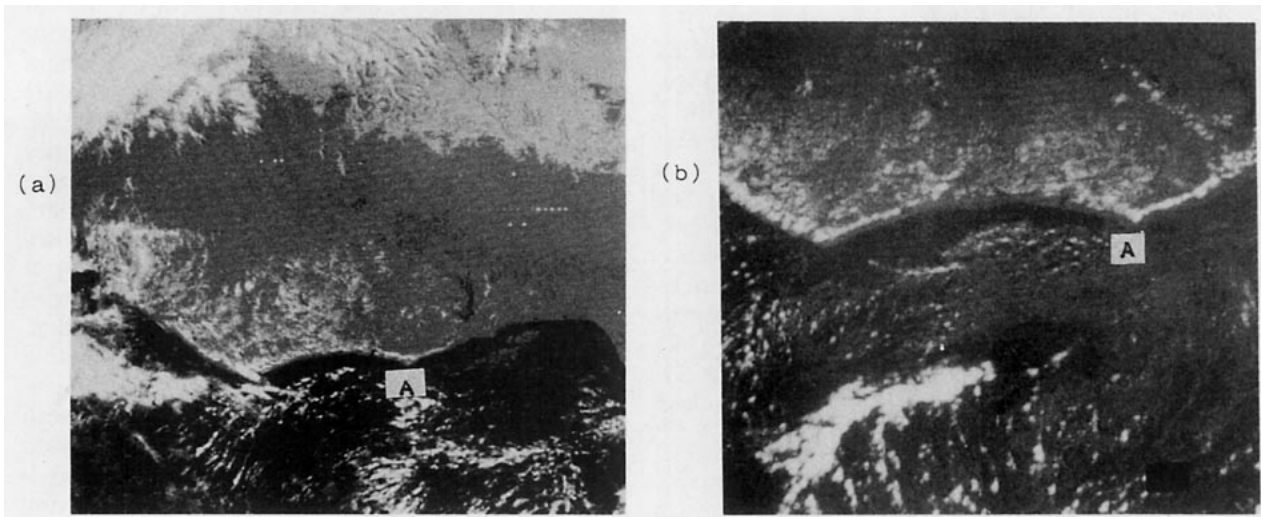

FIG. 2. Meteosat-1 pictures in the visible spectrum: (a) 1430 LST 6 January 1979; (b) 1530 LST 23 January 1979 (A refers to Cape of Three Points).
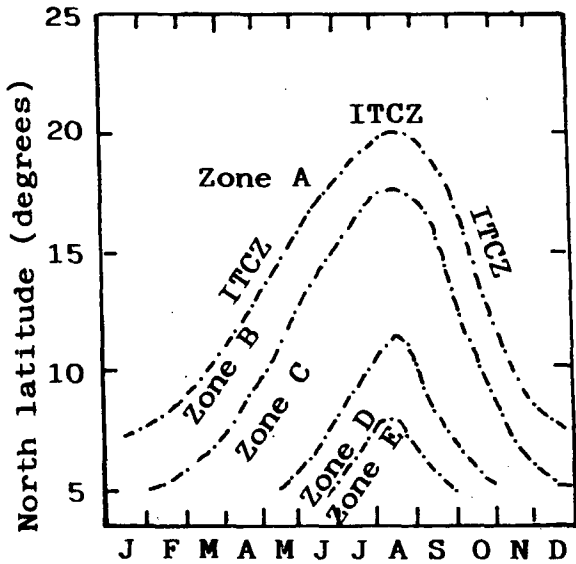
FIG. 3. Intertropical convergence zone displacements in Walker's diagram. Zone A: Saharan cloudless air; zone B: W–SW winds, shallow maritime air, thunderstorms; zone C: intense rainfalls associated with SW monsoon flow; zone D: stable, cold, and very cloudy atmosphere with continuous weak rainfalls; zone E: above the coastal lands only for a short period (July to September), accompanied by low temperatures and only a few rains.
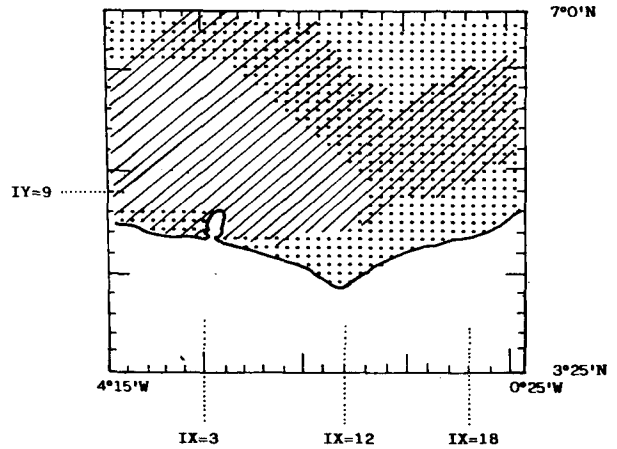

FIG. 5. Vegetation cover at Cape of Three Points: horizontal dashed lines, savannah; solid slashes, forest; mixed dot and solid slashes, mixed (forest and savannah). IX refers to the numbering of grid points along the longitudinal axis. IY refers to the numbering of grid points along the meridional axis.

Regarding the surface forcing parameters, the sea surface temperatures averaged over the first three months of 1979 are shown in Fig. 7, with pools of cold water (24°C) to the east, and warm water (28°C) to the west of CTP. The vegetation cover was parameterized through surface roughness lengths different from forest, savannah, or mixed cover areas (forest and savannah). Micrometeorological studies conducted in the Ivory Coast give some general indication about these roughness lengths, together with soil characteristics

(Cautenet et al. 1985). The main parameters used in our simulations are summarized in Table 1. For both cases, 6 and 23 January 1979, the model is initialized with the corresponding 0000 LST sounding at Abidjan (5.25°N, 4°W).

3. Simulation of two typical situations in the dry season: 6 and 23 January 1979

a. Meteorological characteristics of both simulated situations

The main differences between both days can been depicted from the wind and moisture vertical profiles in Figs. 8a and 8b. In each case, a SW low-level monsoon flux is observed from 0 to 500 m, whereas an easterly flow blows at upper levels, above about 3000
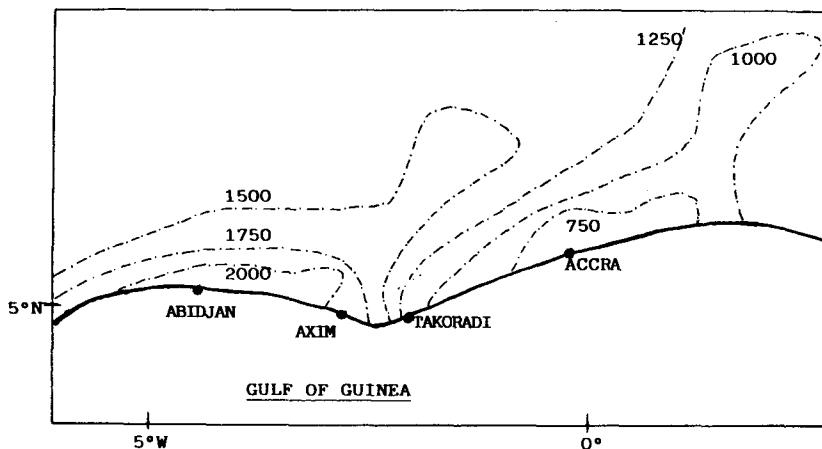

FIG. 4. Annual isohyets (in millimeters) along the Gulf of Guinea at Cape of Three Points (Trewartha 1961).
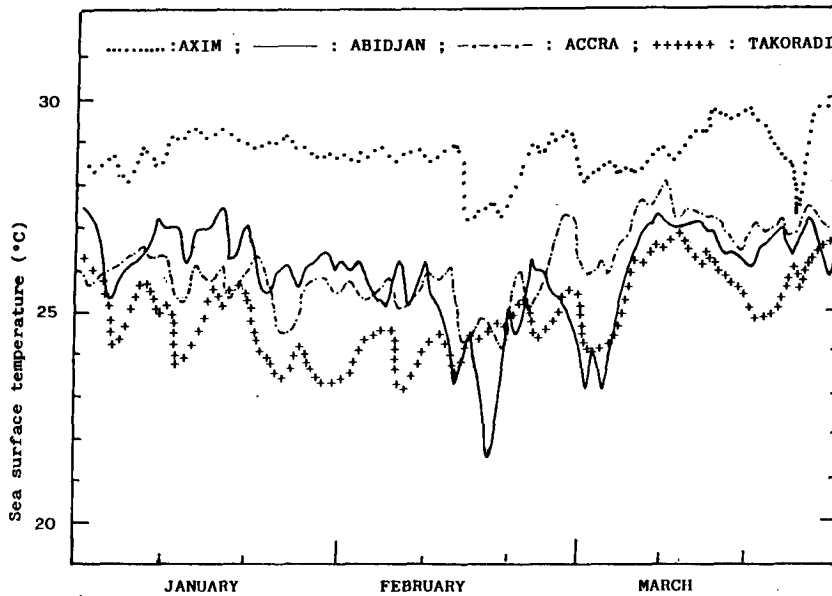
FIG. 6. Evolution of the coastal sea surface temperature (SST) at four stations (Accra, Takoradi, Axim, Abidjan), during the first 3 months of 1979. Note the warmer temperatures at Axim and the lower ones at Takoradi. (Data from Oceanic Research Center at Abidjan).

m. One can see, however, that the low-level flow is stronger on 23 January (6 m s^{-1}) than on 6 January (2 m s^{-1}). The following further significant differences can be noticed:

• The vertical wind shear between 500 and 3500 m is weak on 6 January with a wind rotation from the SW to the E within the southern sector (veering case). Streamflow analysis of 6 January (Figs. 9a, 9b and 9c) shows that the flow direction at 600 m is from the SW, before becoming SE above 1500 m. Furthermore, on 23 January (Figs. 9d, 9e and 9f), the flow direction at 600 m is from the SW, before veering sharply to the

NE at 1500 m, with strong shear between 500 and 1500 m (backing case).

• On 6 January, the southwesterly winds advect very humid air: the 80% relative humidity value is located at about 2400 m (744 hPa) at 1200 LST; on 23 January, although the relative humidity is high below 1100 m (890 hPa), the atmosphere is very dry above this level, and the 80% value is much lower, at 890 hPa (Figs. 8).

• The differences arising between both situations are likely to be governed by weak ITCZ oscillations: the ITCZ moves southward on 6 January, and northward on 23 January (Figs. 10a and 10b).

In brief, the first case (6 January) is characterized by a rather weak vertical wind shear and a humid atmosphere associated with SE winds at intermediate levels between 500 and 2500 m; in the second case, 23
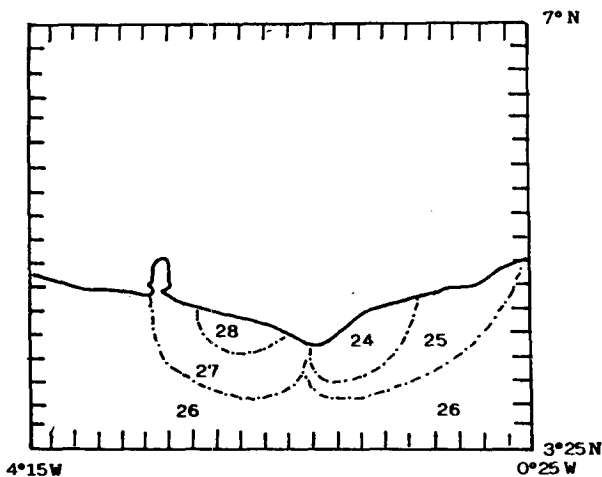

FIG. 7. Sea surface temperatures at Cape of Three Points, averaged over the first 3 months of 1979. (Data from Oceanic Research Center at Abidjan).

TABLE 1. Model input parameters.

| Model parameters	Value
Mean latitude	5°N
Synoptic surface pressure	1010 hPa
Synoptic specific humidity	0.02 g kg^{-1}
Initial planetary boundary layer height	400 m
Albedo	20%
Roughness length z_0 (forest)	90 cm
Roughness length z_0 (savannah)	5 cm
Roughness length z_0 (forest and savannah)	10 cm
Soil heat diffusivity	3 × 10^{-7} m^2 s^{-1}
Soil density	1500 kg m^{-3}
Soil specific heat	1.33 × 10^3 J kg^{-1} K^{-1}
Soil moisture	0.10
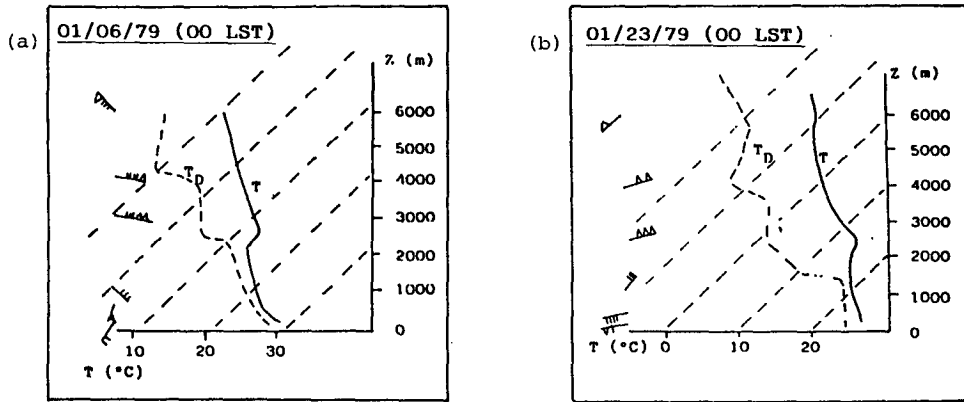
FIG. 8. Vertical temperature, humidity, and horizontal wind profiles at 0000 LST at Abidjan:
(a) 6 January 1979, and (b) 23 January 1979.

January, shear is stronger and winds from the NE above 1500 m are much drier. In both cases, the change in wind direction occurs between 500 and 2000 m.

Radiance isocontours in the visible from Meteosat data (Figs. 11a, b) display different cloud locations in both cases:

• on 6 January convective cells preferentially develop on the western shores of CTP,

• on 23 January the situation is the opposite, with clouds developing on the east shores of CTP.

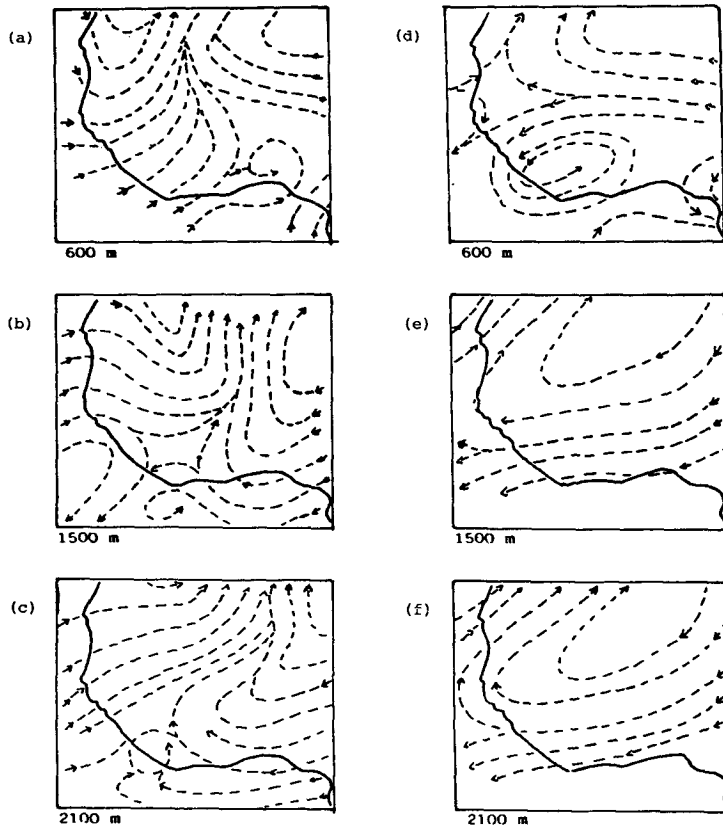From a comparison between the synoptic aerological conditions, it is tentatively inferred that these differ-

FIG. 9. Streamflow analysis at 1100 LST at (a) 600 m, (b) 1500 m, (c) 2100 m
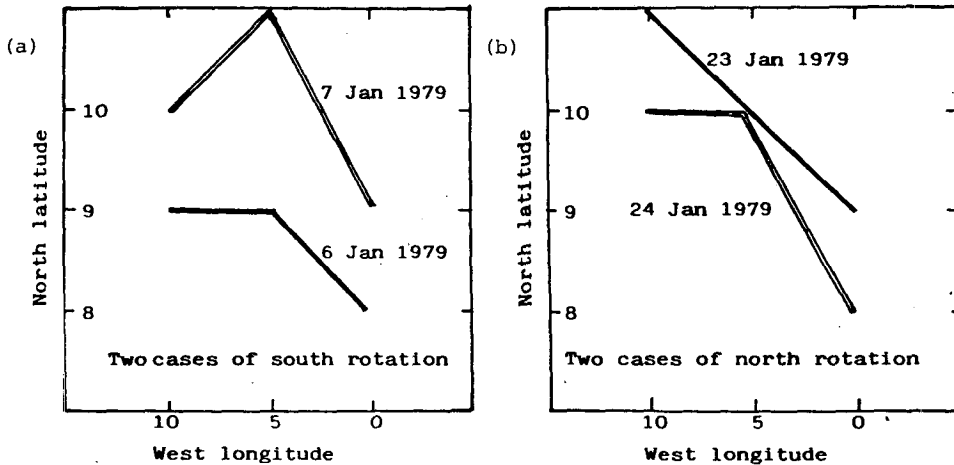on 6 January 1979; (d) 600 m, (e) 1500 m, (f) 2100 m on 23 January 1979.

FIG. 10. Surface location of ITCZ at 1200 LST: (a) 6 January 1979, and (b) 23 January 1979.
The ITCZ moves southwards on 6 January, northwards on 23 January.

ences in cloud location could be attributed to the wind shear between 500 and 2000 m, with veering on 6 January and backing on the twenty-third.

In the following, this hypothesis will be tested through numerical computation of vertical wind field patterns.

b. *The simulation of 6 January 1979*

The model is initialized with the emagram in Fig. 8a. Figure 12a displays the simulated surface (5 m level)

wind field at 1500 LST. One can notice an acceleration across the coastline, together with a change in the direction only on the eastern side of the cape. At the 2000 m level, at 1500 LST (Fig. 12b), one observes a perturbation in the wind field across the coastline. This perturbation is stronger on the east than on the west side. Vertical wind velocities at 1500 LST are the most intense at 300 and 1200 m (Figs. 13a, b), above the center and western part of the cape.

We now proceed to a comparison between the numerical results and selected observational data. First,
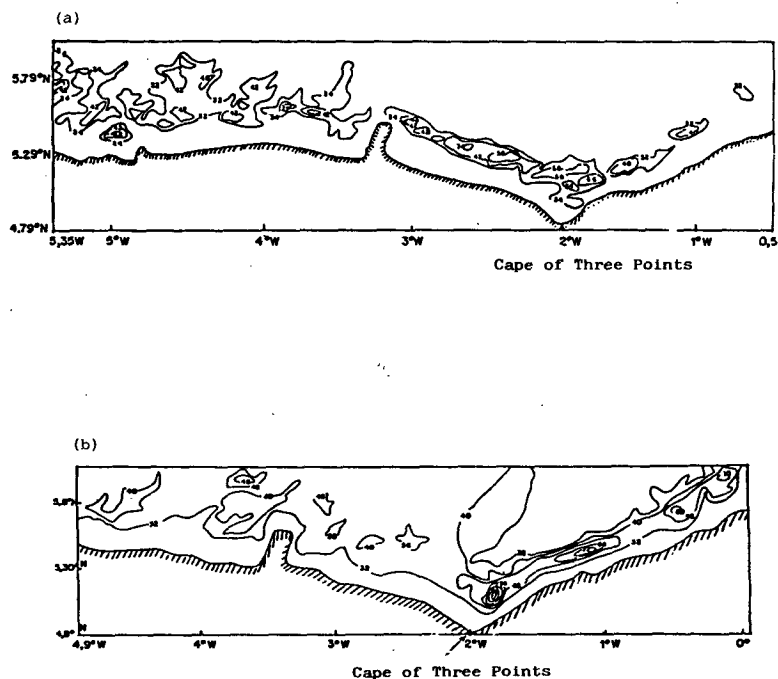

FIG. 11. Radiance isocontours in the visible (in arbitrary count units):
(a) 1430 LST 6 January 1979; (b) 1500 LST on 23 January 1979.
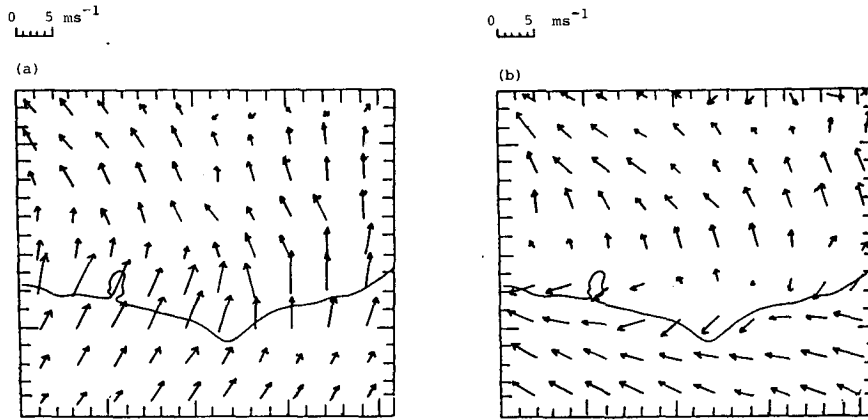
0   5 ms^{-1}

(a)

0   5   ms^{-1}

(b)

FIG. 12. Simulated wind field at 1500 LST on 6 January 1979 at (a) 5 m, and (b) 2000 m.
(Velocity scale included in the figure.)

from the radiance isocontours in the visible on 6 January (Fig. 11a), it appears that the average distance between cloud cells is about 25 km. Such a distance is also found between the cores of the computed vertical wind velocities in Figs. 13, at 300 m (Fig. 13a) and at 1200 m (Fig. 13b). Furthermore, a zone of descending motion is seen at about 80 km inland from the coast, which depicts the northern limit of the sea breeze penetration; on the photosatellites, this distance ranges also between 60 and 80 km at CTP.

Figures 14a, 14b, and 14c display three vertical meridional cross sections at 1500 LST of the meridional (iso-v) and vertical (iso-w) isotachs of the simulated sea breezes. The three meridional planes are defined by their abscissas noted IX: IX = 3 (west of the cape), IX = 12 (center), and IX = 18 at the east. It can be verified that vertical velocities are much stronger (8 cm s^{-1}) at IX = 3, i.e., at the west coast than at IX = 18 (2 cm s^{-1}) on the east coast.

This latter result must be emphasized because it illustrates in this instance the existence of vertical velocities cores much more developed on the western part of CTP than on the east, thus denoting stronger

instability there. This is in agreement with the Meteosat observational data in Fig. 11a.

c. The simulation of 23 January 1979

The model is initialized with the emagram in Fig. 8b. Simulated surface (5 m) wind field at 1500 LST (Fig. 15a) shows once again an acceleration across the coastline but, in contrast to the case of 6 January the change in the mean flow direction at the east coast is not very marked. As a matter of fact, in the lower levels, the SW monsoon flow is stronger than on 6 January thus being less affected by sea breezes. At the 1200 m level and at 1500 LST (Fig. 15b), the strong (backing) wind shear introduced in the simulation is likely to disturb the flow, mainly at the sea–land transition. The vertical velocity field at 300 and 1200 m at 1500 LST (Figs. 16a, 16b) is more intense on the east side of CTP than on the west, with several updraft cores. At 1700 LST at 1200 m on the east coast, simulated updraft cores exhibit a line organization oriented SW–NE (Figs. 17a, 17b) with vertical velocities higher on the east side.
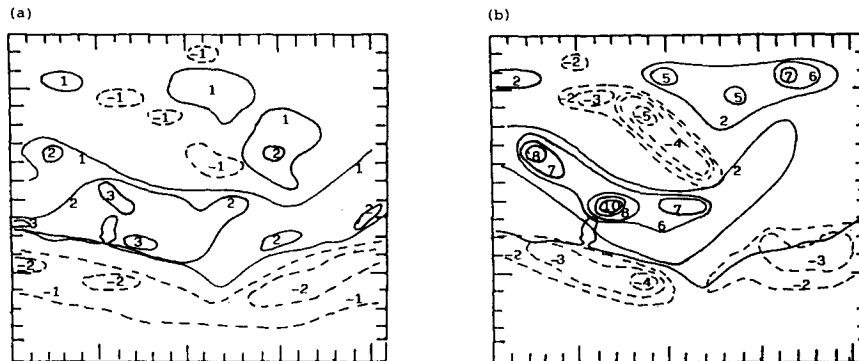
(a)

(b)

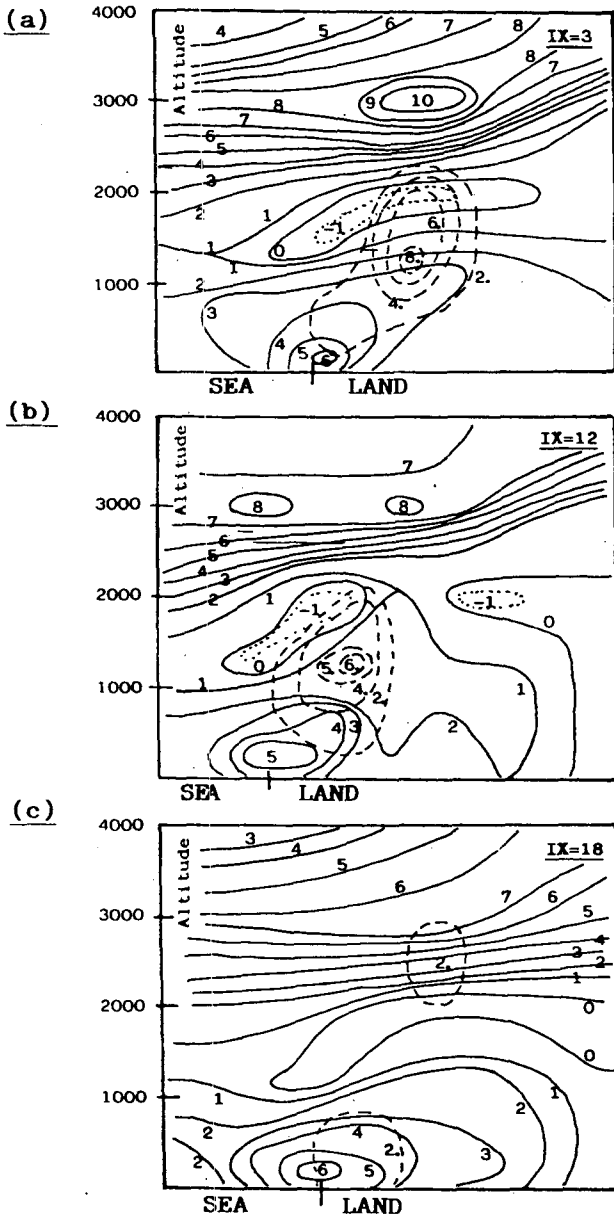FIG. 13. Vertical velocity field (in cm s^{-1}) at 1500 LST 6 January 1979
at (a) 300 m, and (b) 1200 m.

FIG. 14. Cross section of the meridional wind component (solid lines, in m s^{-1}) and vertical velocity (dashed lines, in cm s^{-1}) at 1500 LST 6 January 1979 at (a) IX = 3, (b) IX = 12, and (c) IX = 18. Dotted lines refer to negative values of the meridional wind component.

These results quite agree with the observations; in particular, clouds are more tightly packed above the eastern and central parts of the CTP than on the west.

Regarding 6 January, examination is made in Figs. 18a, 18b, and 18c of the meridional vertical cross sections at 1500 LST of the isotachs in meridional (iso-v) and vertical wind components (iso-w). Three planes are considered, respectively, for the abscissa IX = 3, 12 and 18. One can note that

• the maximum value of the meridional component of the sea breeze (iso-v) is stronger at IX = 18 (7 m s^{-1}) than at IX = 3 (5 m s^{-1});

• the return flow at 2000 m is greater at IX = 3 (−10 m s^{-1}) than at IX = 18 (−8 m s^{-1});

• similarly, the strongest updrafts are found at IX = 18 where they overtake the 2000 m level.

Meteosat photographs (Fig. 11b) show that the distance between the center of the convective cells and the coastline is about 20 km in agreement with the calculations; this may be seen in Fig. 16 which displays the vertical wind velocity pattern. Fig. 11b also shows that, as predicted by the simulation, the maximum updrafts values are found at the east coast of CTP.

4. Preferred location of convective cells

Here, we will concentrate upon the interactions between sea breeze circulations and the synoptic wind shear at the Cape of Three Points. Two typical observed cases (6 and 23 January 1979) have been simulated and a comparison with Meteosat satellite pictures has been performed. The numerical study points out that the vertical wind shear between 500 and 2000 m strongly affects the wind field at the coastline more than anywhere else (Figs. 12 and 15). The PBL flow is strongly influenced by drastic changes in surface roughness across the coastline, together with the wind vertical profiles.

The structure of the sea breeze circulation is affected by changes in the synoptic wind direction (offshore or onshore flow). On 23 January, the sea breeze is confined to low levels with a rather intense return flow; a meridional negative speed core is displayed in Figs. 18a, 18b and 18c. On 6 January, the return flow is very weak (Figs. 14a–c). Both cases are classical examples of onshore and offshore flows; the former generally leads to deep inland penetration with weak return flows, whereas the latter induces a strong return flow with reduced inland penetration (Estoque 1962). The vertical wind velocity field associated with the sea breeze circulation barely overtakes the 2000 m level on 6 January whereas it reaches the 3000 m level on 23 January. It must be noted that on this latter day, the maximum radiance values are much greater (80) in arbitrary count units than on 6 January (66), which is indicative of higher cloud tops (Figs. 11a, b).

In order to assess the role of the wind shear in the release of static instability a convective available potential energy index or CAPE (Green and Dalu 1980) has been estimated. By definition,

$$\text{CAPE} = mg\, h\, \delta q / C_p \theta_0$$

where m is the mass of an air parcel rising to level h, after taking a diabatic energy input δq, its potential temperature being initially equal to θ_0. CAPE is directly
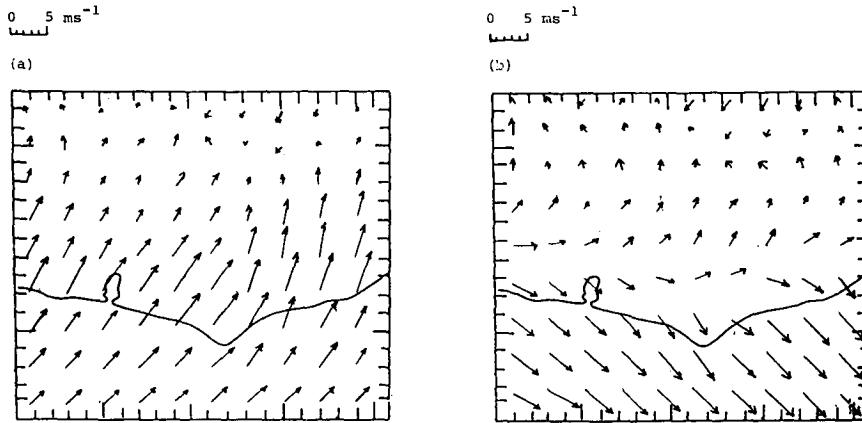
FIG. 15. The simulated horizontal wind field at 1500 LST on 23 January 1979 at (a) 5 m, and (b) 2000 m. (Velocity scale included in the Fig.)
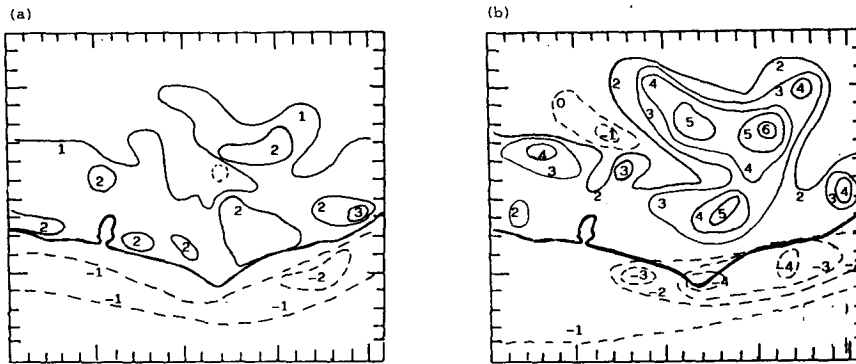
FIG. 16. Vertical velocity field (in cm s^{-1}) at 1500 LST on 23 January 1979 at (a) 300 m, and (b) 1200 m.
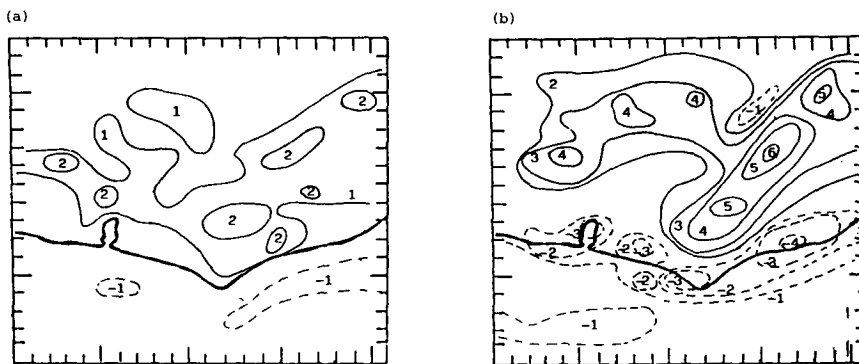
FIG. 17. Vertical velocity field (in cm s^{-1}) at 1700 LST 23 January 1979 at (a) 300 m, and (b) 1200 m.

linked to the probability of convection. In practice, we have instead evaluated the ratio $\eta = H/\theta_0$, proportional to CAPE, where H is the calculated surface sensible heat flux. A longitudinal profile of η over CTP at the coordinate IY = 9 (see Fig. 5) is given in Fig. 19. In-

stability is almost symmetrically distributed across the area, its maximum occurring at the coasts. Obviously, this symmetry in η is not sufficient to predict where convection is to develop preferentially, both coasts being a priori favored places. Numerical experiments
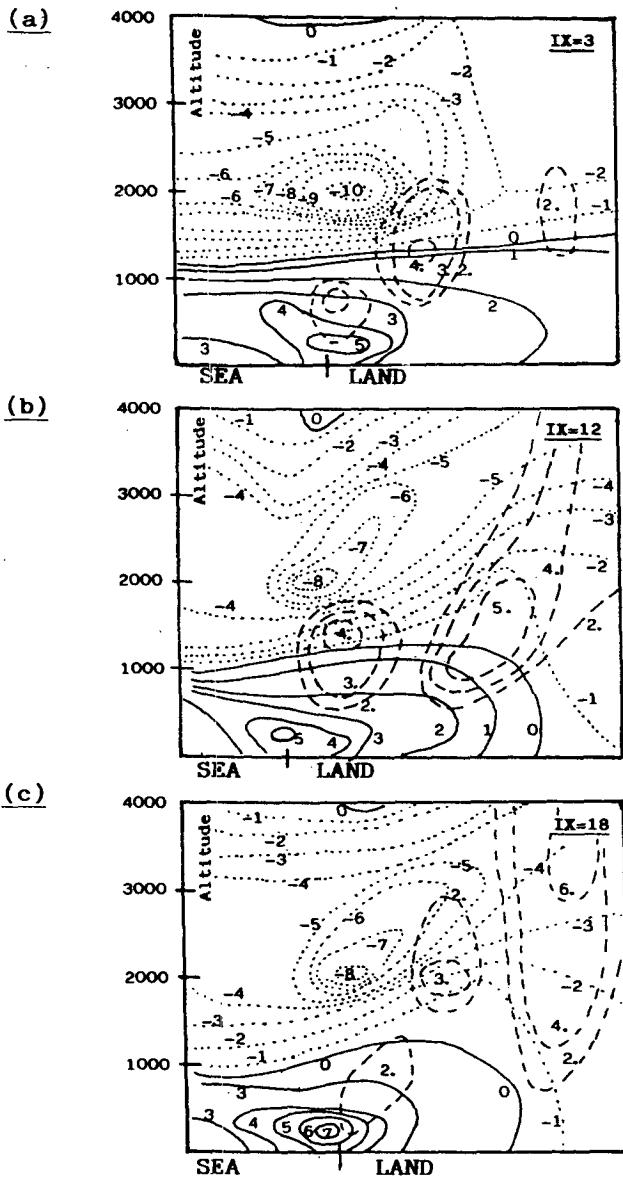
(a)

(b)

(c)

FIG. 18. Cross section of the meridional wind component (solid lines, in m s^{-1}) and vertical velocity (dashed lines, in cm s^{-1}) at 1500 LST 23 January 1979 at (a) IX = 3, (b) IX = 12, and (c) IX = 18. Dotted lines refer to negative values of the meridional wind component.

as well as observations point out that this is not the case: on 6 January, convective clouds concentrate at the west of CTP but at the east on 23 January. The wind direction in the 500–2000 m layer seems to appear as a prominent factor for cloud cell location. Though both airflows are sheared, it is possible to define an average southeasterly flow on 6 January whereas on 23 January the average wind comes from the northwest. In order to explain the mechanism through which wind shear acts on circulation, we have assumed that the

wind profiles are equivalent to an average flow, a SE flow for wind veering and a NW flow for backing, respectively. We have simulated both cases using these unsheared average flows instead of sheared real ones. Although for the sake of brevity, the detailed results are not given here, we note that in the former case (i.e. 6 January), simulation leads to more instability on the west coast than on east; however, in the latter case, (23 January) greater instability was found on the opposite coast. These latter simulations suggest that the vertical shear acts as a wind averaged over the 500–2000 m layer, the average direction being the key factor. This is in agreement with Pielke's (1974) investigations over Florida, a peninsula which has an axis with approximately the same N–S orientation as CTP. This author has simulated the wind direction effect of a constant unsheared geostrophic flow, pointing out that a SE flow induces enhanced cloud convection on the west coast with the opposite situation occurring with a SW flow.

5. Conclusions

Equatorial sea breezes have been studied at Cape of Three Points which is characterized by strong contrasts in pluviometry, vegetation cover and sea surface temperatures between its eastern and western shores. Two typical situations during the 1979 dry season have been selected for simulation. In the first case, 6 January, the wind profile displays a veering between the surface and the AEJ, and a backing in the second case, 23 January. We have shown that the equivalent average wind direction in the 500–2000 m layer is likely to be the prominent factor for cloud cells location, with SE flow
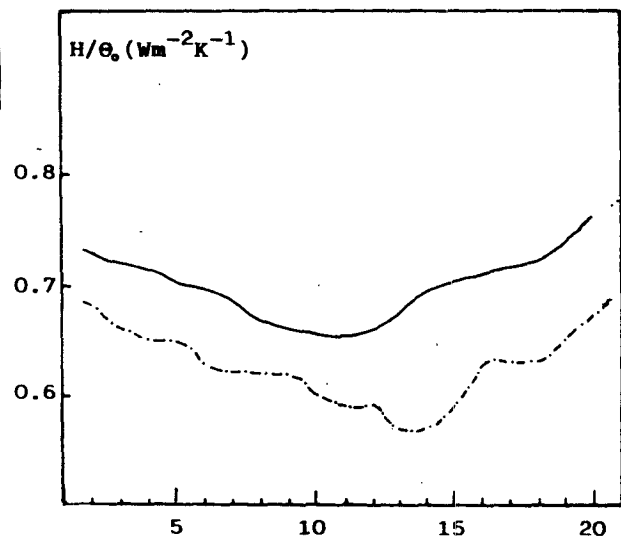

FIG. 19. Latitudinal cross-section of $\eta = H/\theta_0$ at Cape of Three Points at the ordinate IY = 9 (cf. Fig. 5). (Solid line for 6 January 1979; dashed-dotted line for 23 January 1979).

in case of wind veering (6 January) and a NW flow for backing (23 January). In both typical cases, rather good agreement has been found between observations and the numerical results. We want to emphasize in this particular study the interest of numerical simulation in equatorial poor data-covered regions.

REFERENCES

Burpee, R. W., 1972: The origin and structure of easterly waves in the lower troposphere of North Africa. *J. Atmos. Sci.,* **29,** 77–90.

Cautenet, G., Y. Coulibaly and Ch. Boutin, 1985: Calculation of ground temperature and fluxes by surface models: A comparison with experimental data in the African savannah. *Tellus,* **37B,** 64–77.

Estoque, M. A., 1962: The sea breeze as a function of the prevailing synoptic situation. *J. Atmos. Sci.,* **19,** 244–250.

Green, J. S. A., and G. A. Dalu, 1980: Mesoscale energy generated in the boundary layer. *Quart. J. Roy. Meteor. Soc.,* **106,** 721–726.

Hong Yan, and R. A. Anthes, 1987: The effect of latitude on the sea breeze. *Mon. Wea. Rev.,* **115,** 936–956.

Mahrer, Y., and R. A. Pielke, 1978: A test of an upstream spline interpolation technique for the advective terms in a numerical mesoscale model. *Mon. Wea. Rev.,* **106,** 818–830.

Pielke, R. A., 1974: A three-dimensional numerical model of the sea breezes over South Florida. *Mon. Wea. Rev.,* **102,** 115–139.

Rennick, M. A., 1976: The generation of African waves. *J. Atmos. Sci.,* **33,** 1955–1969.

Trewartha, G. T., 1961: *The Earth's Problem Climates.* The University of Wisconsin Press, 385 pp.